

CityGen: Infinite and Controllable 3D City Layout Generation

Jie Deng^{1,*} Wenhao Chai^{2,*†} Jianshu Guo^{1,*} Qixuan Huang¹ Wenhao Hu¹
 Jenq-Neng Hwang² Gaoang Wang^{1,✉}

¹ Zhejiang University ² University of Washington

* Equal contribution † Project lead ✉ Corresponding author

<https://reself.github.io/CityGen/>

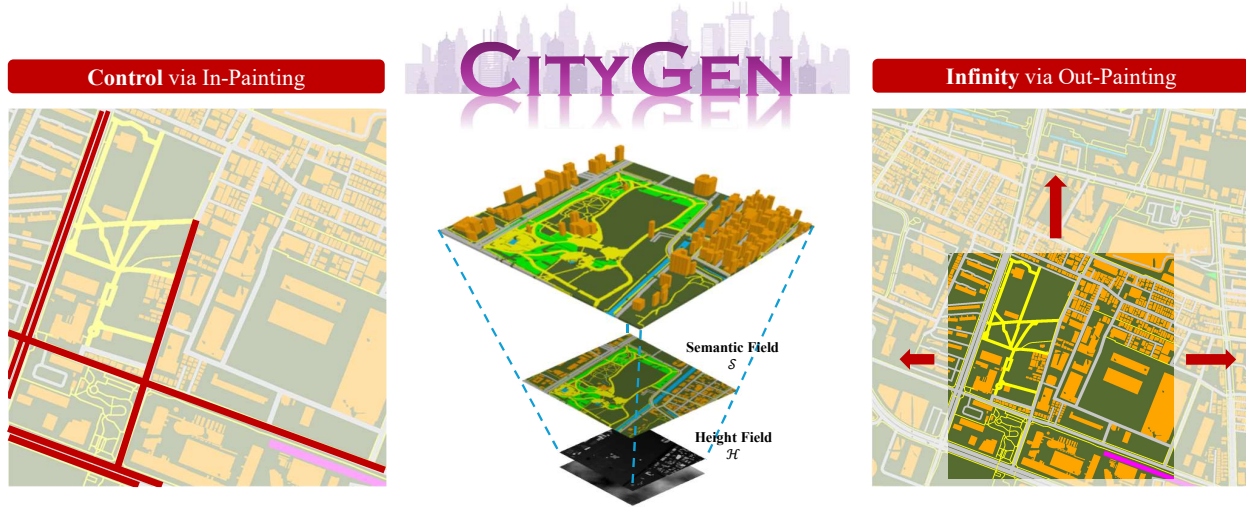


Figure 1. **CityGen** is a novel framework for infinite, controllable and diverse 3D city layout Generation. We propose an auto-regressive out-painting pipeline to extend the local layout to an infinite city layout. Moreover, we utilize a multi-scale refinement network to generate fine-detailed and controllable semantic field.

Abstract

City layout generation has recently gained significant attention. The goal of this task is to automatically generate the layout of a city scene, including elements such as roads, buildings, vegetation, as well as other urban infrastructures. Previous methods using VAEs or GANs for 3D city layout generation offer limited diversity and constrained interactivity, only allowing users to selectively regenerate parts of the layout, which greatly limits customization. In this paper, we propose *CityGen*, a novel end-to-end framework for infinite, diverse and controllable 3D city layout generation. First, we propose an outpainting pipeline to extend the local layout to an infinite city layout. Then, we utilize a multi-scale diffusion model to generate diverse and controllable local semantic layout patches. The extensive experiments show that *CityGen* achieves state-of-the-art (SOTA) performance under FID and KID in generating

an infinite and controllable 3D city layout. *CityGen* demonstrates promising applicability in fields like smart cities, urban planning, and digital simulation.

1. Introduction

3D virtual city generation is a rising task in computer vision. Creating realistic, three-dimensional digital copies of urban environments enables the exploration of various architectural designs and infrastructure scenarios. In all city generation tasks, the generation of the city layout stands out as the initial and one of the most crucial steps. During the past years, researchers have made various attempts to generate realistic city layouts, including procedural modeling [17, 44, 48, 54, 62], which progressively creates city layouts based on predefined rules and algorithms, and image-based modeling [5, 11, 12, 22, 28, 58], which generate layouts using images, such as aerial, satellite, and street im-

ages. Although these methods are effective for city layout generation, they typically require prior knowledge.

Researchers have explored leveraging VAEs [34], GANs [37], and diffusion models [33] for layout generation in diverse domains but these methods representing object layouts as bounding boxes have limited applicability to complex city scenes. Recently, [43, 61] proposed to represent city layouts as semantic masks. However, these methods lack diversity and controllability, and the generated layouts lack long-range global structural coherence.

To address these problems, we propose CityGen, an end-to-end model to generate infinite, coherent, and controllable 3D layouts for virtual cities. We utilize an efficient representation for 3D city layout which only consists of a semantic field and a height field [19]. To generate the semantic field, we first employ diffusion models [30] to create a local semantic block and then construct an infinite expansion model to extend it into a global semantic field. It is noteworthy to highlight that we train the diffusion model in the one-hot space, as we represent the semantic map as a one-hot vector. This training approach exhibits robust performance when compared with the conventional RGB image space. After that, we develop a multi-scale refinement framework that progressively up-samples all local semantic blocks and combines them to form a high-resolution coherent global semantic field. The motivation behind the multi-scale refinement framework is to integrate the large-scale global semantics with the fine-grained details at a lower scale. Additionally, we design a user-friendly scheme to facilitate user control over the generation of layouts. Given any user sketches of a city layout, our model can produce high-quality, diverse samples devoted to user customization. To synthesize a height field for a given semantic field, we separate classes and model heights for each class according to elevation patterns we observe in the real world. We further segment buildings into instances to enable precise and diverse height assignments for each building instance. We combine these submodules to provide realistic, infinite, and diverse 3D city layouts. Our main contributions can be summarized as follows:

- We propose CityGen, an end-to-end framework to generate infinite, controllable and diverse 3D city layouts.
- We propose a multi-scale refinement framework that can progressively refine the low-quality global semantic field. This framework is envisioned to simultaneously attain both quality and diversity while ensuring minimal computational overhead.
- We design a user-friendly scheme that enables users to guide the generation of customized city layouts tailored to user design goals through simple sketching interactions.

2. Related Works

2.1. 3D Scene Generation

3D Scene Generation focuses on the creation of efficient 3D representations of scenes, with a primary categorization into indoor [21, 23, 49, 53] and outdoor scenes [13, 20]. Outdoor scenes further encompass natural [15, 21, 26] and urban [52] environments. Scenes can be represented explicitly using voxels [35, 39], point clouds [18, 32], occupancy [56, 59], or implicitly using Neural Radiance Fields (NeRF) [55, 57, 60]. Recently, notable advancements have been made in the generation of infinitely extending natural [19, 40, 45] and urban scenes [43, 61]. More recently, InfiniCity [43] generates BEV map and uses 3D octree-based voxel completion for scene construction, and CityDreamer [61] focuses on rendering after city layout creation. However, those works have limited considerations for diversity and user-control in 3D city layout generation, which are further explored in this paper.

2.2. City Layout Generation

The generation of city layouts involves multifaceted considerations within the realm of urban planning, encompassing aspects such as road networks, land use zoning, and the precise placement of buildings. These city layouts can be created through a spectrum of methods, ranging from rule-based manual design [7, 10], semi-automated processes via procedural generation [24, 25] using tools like CityEngine [2] and Unreal Engine [4], to fully automated techniques utilizing deep learning methodologies [43, 61]. The most similar approaches to ours are diffusion model-based methods like [27] and [33]. However, their representation of layouts as bounding boxes limits their freedom to capture complex shape of objects in city scenes. In comparison to established techniques, our approach showcases a more diversified and higher-quality generation.

2.3. City Scene Image Synthesis

The synthesis of city scene images presents a formidable challenge, given the inherent intricacies of urban landscapes compared to other natural scenes. Previous efforts employing techniques like Neural Radiance Fields (NeRF) [19, 43, 61], have demonstrated the capability to generate city scenes. However, these methodologies are associated with prolonged computational duration. There are also works tried to edit or generate consistent results in video [14] or 3D [47] via ControlNet [63], but they do not work well under specific urban scenarios. These works typically use datasets like KITTI [41] and nuScenes [9] for city scene image synthesis. We finetune Stable Diffusion [50] by the Low-Rank Adaptation [31] on MatrixCity [38] dataset to generate realistic and diversified city scene images through ControlNet control.

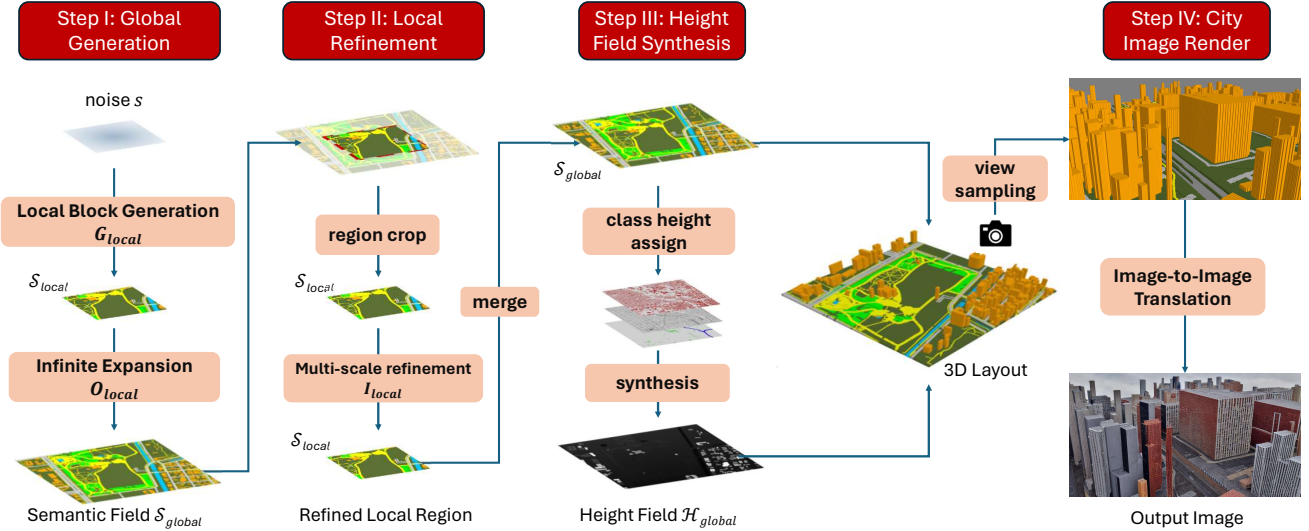


Figure 2. **CityGen Framework.** In the initial step, we sample a local block from noise and extend it infinitely through the auto-regressive outpainting process. Subsequently, we iteratively refine the global semantic field to achieve a more nuanced and polished global field. Following the refinement, height values are assigned to each class. After that, we integrate the semantic field with the height field to synthesize the 3D layout. Finally, by employing an image-to-image approach, we can effectively synthesize diverse city scenes.

3. Methodology

3.1. BEV Layout Representation

We aim to explicitly represent the 3D city layout while achieving efficiency and expressiveness. Instead of voxel or point cloud-based 3D representation, we utilize an efficient bird’s-eye-view (BEV) scene representation only consisting of a semantic field \mathcal{S} and a height field \mathcal{H} . We build a two-stage generation pipeline under our BEV layout representation: 1) the infinite and controllable semantic field generation and 2) the corresponding height field synthesis.

3.2. Semantic Field Generation

The semantic field \mathcal{S} represents the semantic labels (*e.g.* roads, buildings, vegetation, and *etc.*) of each position, which is a one-hot coding map of resolution $H \times W \times C_s$, where H, W are height and width, and C_s is the number of semantic labels. Generating the full semantic field of a city at once leads to intractable complexity and insufficient detail. Thus, we initiate the semantic field by generating a local block at a low resolution and then use inpainting to refine details and outpainting to extend it to infinity.

Block Generation. Considering the excellent generation capabilities of the diffusion models in terms of in-painting and out-painting, we train one-hot diffusion models $G_B(\cdot)$ as the foundational models for block generation. To be specific, we generate semantic field \mathcal{S} with C_s channels. During training, $G_B(\cdot)$ is applied as the denoising network to

predict the noise, which is optimized by minimizing the following objective in Equation 1:

$$\min_{\theta_{G_B}} \mathbb{E}_{\epsilon \sim \mathcal{N}(0, I), t \sim \mathcal{U}(1, T)} \|\epsilon - G_B(s_t, t)\|_2^2, \quad (1)$$

where s_t is the noisy semantic field at timestep t and θ_{G_B} are the parameters of G_B . After that, the noise s of shape $H \times W \times C_s$ is randomly sampled in the inference process. We then convert the denoising result back to a one-hot semantic field \mathcal{S} by applying the $argmax(\cdot)$ function to each entry. We train three block generation models with images of three scales, and all images are down-sampled to the same lowest resolution during training.

Multi-scale Refinement via Inpainting. The semantic field generated from the infinite outpainting pipeline can be converted back to its original resolution by resizing. However, the interpolation process creates artifacts and blurry boundaries between objects. To resolve these issues, we designed a cascaded refinement network that progressively refines the resized results. We take the two-block generation models trained with images at lower scales and build an inpainting refined model for each scale. Each inpainting model’s denoising work $I_B(\cdot)$ inherits the architecture of the block generation model’s denoising network $G_B(\cdot)$ and is initialized with $G_B(\cdot)$ ’s weights. The only difference is that it takes an extra binary mask m_{in} as input, which is used to control the content we want to repaint for refinement. We observe that during resizing, artifacts and inconsistency mainly occur at the edges of objects. Therefore,

we apply a canny edge detector to find the edges of objects and set $m_{in} = 0$ at neighboring pixels of edges to repaint regions nearing edges and $m_{in} = 1$ at regions we want to preserve. At each denoising step t , we preserve consistency between original regions s_{ori} and refined regions s_{ref} using blended diffusion [6] illustrated in Equation 2, in which \odot denotes element-wise multiplication.

$$s_t = s_{t,ori} \odot m_{in} + s_{t,ref} \odot (1 - m_{in}) \quad (2)$$

The training objective for each inpainting model is also similar to the block generation model, as shown in Equation 3:

$$\min_{\theta_{I_B}} \mathbb{E}_{\epsilon \sim \mathcal{N}(0, I), t \sim \mathcal{U}(1, T)} \|\epsilon - I_B(s_t, t, m_{in})\|_2^2, \quad (3)$$

where θ_{I_B} are the parameters of I_B .

User-customization via Inpainting. Our multi-scale refinement model allows for natural and intuitive interactions with users. Given a coarse user sketch of any size, we first crop it into patches at scales of the inpainting models, then convert each patch to an incomplete semantic field patch S'_{local} . After that, S'_{local} can be fed into an inpainting model to get a complete semantic layout S_{local} .

Infinite Generation via Outpainting. We build our infinite generation pipeline upon the block generation model trained with images at the largest scale. We choose to perform outpainting on the largest scale since a known problem of the auto-regressive model is that it tends to predict repeated contents. While the samples from the largest scale contain the richest semantic information, it will help prevent the auto-regressive model from generating repeated contents and give the most diverse results. The outpainting model’s denoising network has the same architecture and training objective as the inpainting model’s denoising network, and they only differ in mask design. The outpaint model’s mask m_{out} is also a binary mask but $m_{out} = 1$ at known regions and $m_{out} = 0$ at outpainting target positions. By sliding the outpainting mask m_{out} in various directions using various overlapping ratios with known regions, we can progressively outpainting existing local semantic field into a global semantic field of desired size. During the outpainting procedure, we also use blended diffusion [6] to ensure smooth connection between known regions and outpainted regions.

3.3. Height Field Synthesis

Given a semantic map S , we separate classes and generate a height field for each class. In theory, a semantic field and its corresponding height field can be generated simultaneously during the block generation phase through a

parallel network with a multi-task loss as in [43, 61]. However, during our experiments, we note such kind of generation can only at most guarantee consistency between a semantic field and the height field in a local block. As the autoregressive pipeline proceeds, the height field and semantic field become less consistent. Meanwhile, in practice a building’s rooftop should be relatively flat but the generated height field has irregular points since the OSM [3] data’s height fields used for training contain irregular or mislabeled points. A few irregular points might be tolerable when visualized in 2D space but when we convert it to 3D visualization, the inconsistency becomes more obvious. Moreover, since building heights manifest notable diversity while other types (terrain, vegetation, road, and *etc.*) pertain to negligible elevation variations, it is not appropriate to model all type’s heights using one distribution. As a result, we synthesize height fields for each class separately.

We create a binary mask M_i for each class C_i such that $M_i = 1$ at indices where $S = i$ and $M_i = 0$ at other indices. In the real world, height variations of the terrain, vegetation, and water surface exhibit a relatively uniform pattern, hence we use a different simplex noise [46] to synthesize a height field for each class. For traffic roads, footpaths, and rails, since their elevations are even more flat due to human design, we assign fixed heights to each class and overlaid them above terrain or vegetation by summing their heights at all locations. While buildings tend to have more variations in heights, we isolate each building instance by detecting connected components, and generating a unique height for each instance. For each building instance, we first randomly sample a building type from a set of choices such as townhouse, apartment, *etc.* Each building type is associated with a Gaussian distribution characterized by distinct mean and variance parameters. Subsequently, the height of the selected building is determined by randomly sampling a value from the Gaussian distribution corresponding to the chosen building type.

3.4. 3D Layout Construction

Given a semantic field S representing the semantic label of the highest surface point in the vertical direction, and the corresponding height field \mathcal{H} representing the highest elevations for all points, we can construct a 3D city layout by lifting each point to its corresponding height as shown in the middle of Figure 1. In this procedure, we let all points on the same vertical axis share the same semantic label.

3.5. City Scene Image Synthesis

Following the construction of the 3D city layout, we proceed to finetune the Stable Diffusion [50] model on the MatrixCity [38] dataset through Low-Rank Adaptation (LoRA) [31] method in order to synthesize authentic city scene images. After finetuning, we can proficiently inte-

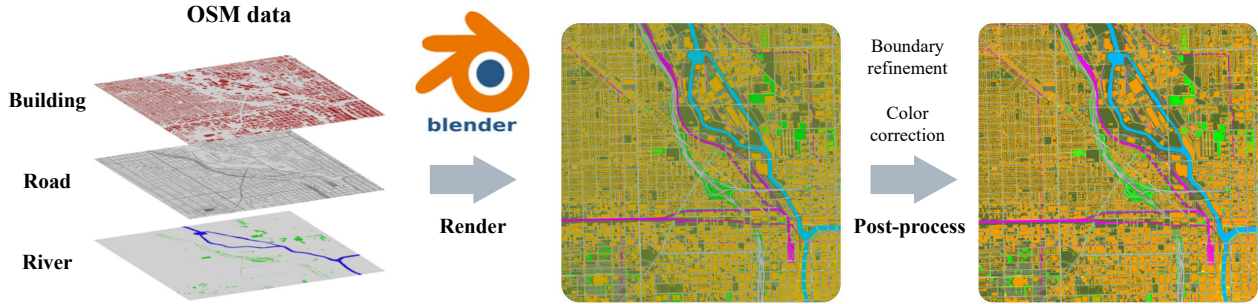


Figure 3. **OSM Dataset Processing Pipeline.** We first populate 3D city models for real-world cities with various geospatial elements like buildings, roads, bodies of water, and vegetation. Subsequently, we render the 3D city models with Blender [1]. Then, we develop a post-processing pipeline that consists of boundary refinement and color correction.

grate the pre-trained ControlNet [63] to produce city scene images that align with the underlying 3D layout structure.

Since LoRA provides a memory-efficient and accelerated technique for diffusion models, we adopt LoRA to finetune the network weight residuals instead of the entire weights. Specifically, for a layer l with weight matrix $W \in \mathbb{R}^{n \times m}$, the residual ΔW is finetuned. A key aspect of LoRA is the decomposition of ΔW matrix into low-rank matrices $A \in \mathbb{R}^{n \times r}$ and $B \in \mathbb{R}^{r \times m}$: $\Delta W = AB$. We apply LoRA for the cross-attention and self-attention layers of the stable diffusion network. After LoRA finetuning, the model can learn to generate high-quality city scenes. Some examples are shown in Figure 8. Given sampled views of the generated 3D layouts, realistic synthesis results can be attained.

4. Dataset

Layout Generation Our training data for 3D layout generation comes from OpenStreetMap (OSM) [3], a free open geographic database updated and maintained by a community of volunteers via open collaboration. We first populate 3D city models for real-world cities with various geospatial elements like buildings, roads, bodies of water, and vegetation. Subsequently, we render the 3D city models with Blender [1]. After that, we set the camera configurations to get orthogonal aerial projections of the terrain models of size 8192×8192 with a pixel-to-meter ratio of 2:1 to represent an area of 4096×4096 m² in the real world. During the rasterization process, the RGB values of 2D views undergo subtle alterations, particularly at the boundaries between distinct object types, attributable to rendering artifacts. To resolve these artifacts, we develop a post-processing pipeline that consists of boundary refinement and color correction. This procedural requirement is essential due to the pivotal role of colors in representing class labels within our research framework. Any misalignment in colors can potentially lead to inaccurate representations of class information, introducing a risk of false

indications. Subsequently, we crop these high-resolution projections to generate patches of optimal sizes including 128×128 , 256×256 , and 512×512 to facilitate the training of models at all scales. We demonstrate the complete processing pipeline in Figure 3.

Image Synthesis For city scene image synthesis, we directly use the MatrixCity [38] dataset for training, where the MatrixCity dataset contains 67k aerial images and 452k street images from two city maps of total size 28km^2 .

5. Experiments

Implementation Details We train three block generation models with training images at three scales: 128×128 , 256×256 , and 512×512 . All images are down-sampled to 128×128 during training and the results are up-sampled to their original size during inference. Both down-sample and up-sample use the nearest neighbor interpolation. Each block generation model is a Denoising Diffusion Probabilistic Model (DDPM) [30] and we use UNet [51] as the denoising network. All training and experiments are conducted using four NVIDIA Ampere Tesla A40 GPUs. The outpainting model is trained with 512×512 images and the two inpainting models are trained with 256 and 128 images, respectively. The outpainting and inpainting models are initialized with the weights of the block generation models trained at corresponding image scales and we add $C_s + 1$ extra input channels initialized with zero weights to the first *conv.in* layer of the UNet in the channel dimension, such that it takes $\text{Concat}(m, m \odot S_t, S_t)$ as input, where $\text{Concat}(\cdot)$ stands for concatenation in the channel dimension. We use Adam [36] as the optimizer for training all models. We use a learning rate of 1×10^{-4} for all block generation models and 1×10^{-5} for all inpainting and outpainting models.

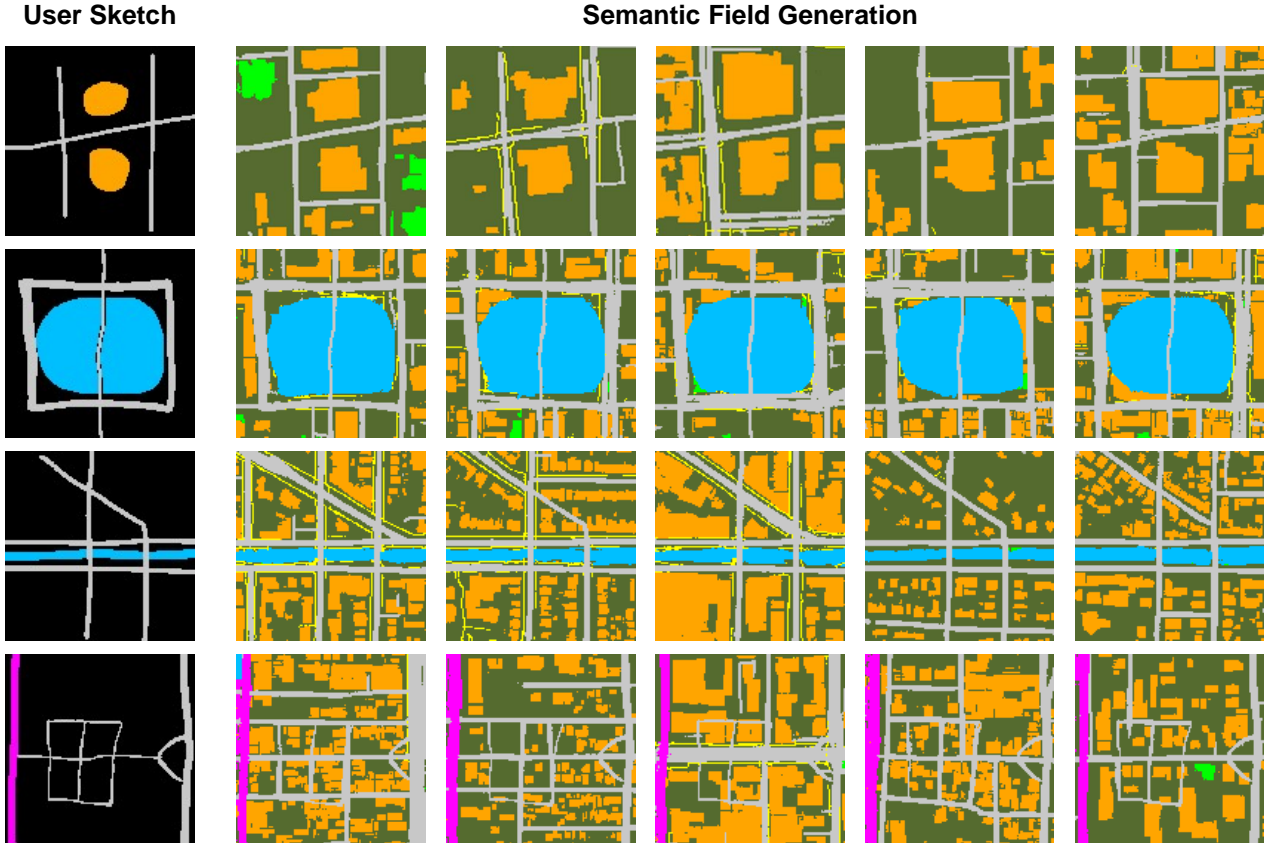


Figure 4. **User Control Results** Given user controls as sketches, we generate diverse and faithful semantic fields.

Method	FID (\downarrow)	KID (\downarrow)
InfiniCity [43]	80.35	0.0875
CityDreamer [61]	124.45	0.123
CityGen (ours)		
BG ₁₂₈	20.18	0.0221
BG ₂₅₆	28.92	0.0290
BG ₅₁₂	61.38	0.0595

Table 1. **Quantitative comparison on block generation.** CityGen models substantially outperforms other methods in FID and KID (both the lower the better).

Evaluation Metrics To evaluate the performance of all models quantitatively, we adopt two evaluation metrics: Kernel Inception Distance (KID) [8] and Fréchet Inception Distance (FID) [29].

Block Generation Models We first evaluate the performance of our block generation models trained at three image scales: BG₅₁₂, BG₂₅₆, BG₁₂₈ and compared them with the state-of-the-art method InfiniCity [43] both qualitatively

Method	FID (\downarrow)	KID (\downarrow)
Out ₅₁₂	15.38	0.0120
In ₂₅₆	22.25	0.0171
In ₁₂₈	27.33	0.0215

Table 2. FID and KID for inpainting and outpainting models.

and quantitatively. Since InfiniCity is not open-sourced, we compare our layout generation method with its layout generation method InfinityGAN [42]. To ensure fair comparison, we train InfinityGAN with our dataset in RGB space with the same settings used in the InfiniCity paper. We train InfinityGAN for 800,000 iterations and select the model with best FID (epoch = 231,000). In Figure 6, we show both raw sampled results and results after mapping the color of each pixel to its nearest neighbor in the predefined palette for InfinityGAN, and compare them with sampled results from our three block generation models. It is notable that the color conversion for InfinityGAN samples create undesirable artifacts near boundaries of objects (highlighted with red boxes). In Table 1 we perform quantitative compar-

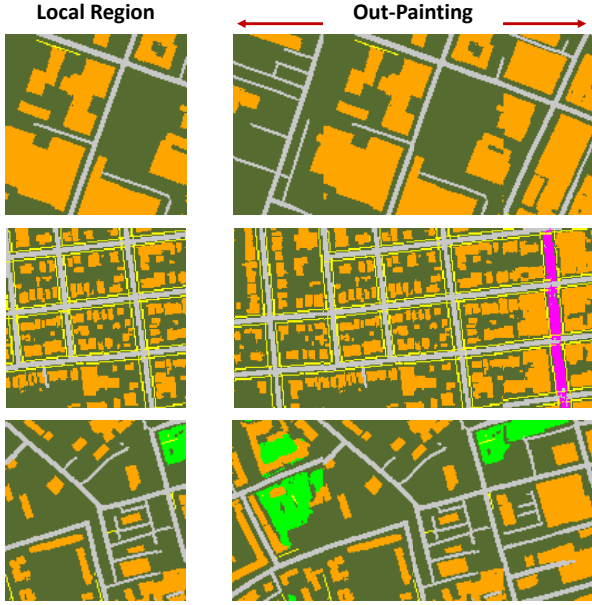


Figure 5. **Infinity Expansion.** Given local regions, we can expand them infinitely.

isons by calculating the FIDs and KIDs for InfinityGAN and compare them with our models. We sample 10,000 samples from each model and randomly sample 10,000 real images when calculating FID and KID. We also compare our results with a concurrent work CityDreamer [61], however, since neither CityDreamer nor its layout generation method [16] is open-sourced, we directly list its quantitative results here. Since CityDreamer also used the OSM dataset for training, we believe training with our dataset would lead to negligible variations in the evaluated results. From both qualitative and quantitative comparison results, we draw conclusion that our block generation models trained with images at three scales substantially outperform other methods in terms of city layout generation.

Inpainting and Outpainting Models We also evaluate our two inpainting models and the outpainting model. To generate samples from these models, we draw samples from the test set, mask them with a random ratio $\sigma \in (0.1, 0.9)$ and let the inpainting/outpainting models repaint masked regions. The inpainting masks are created randomly, while outpainting masks are designed to have rectangular unknown regions near the boundaries of the semantic field. The results are shown in Table 2. We observe that the inpainting and outpainting models have significantly lower FIDs and KIDs than the block generation models although they were trained using same images. We believe this is because during inpainting or outpainting, part of the images were treated as known regions for the models, such that

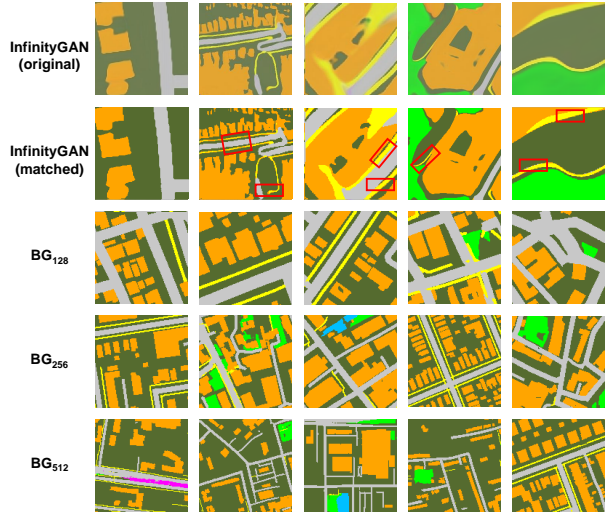


Figure 6. **Patch Samples.** Samples from all block generation models, (1). InfinityGAN (2). InfinityGAN results after nearest neighbors color mapping (3). Our Block Generation model trained with 128×128 images (4) Block Generation model trained with 256×256 images (5) Block Generation model trained with 512×512 images.

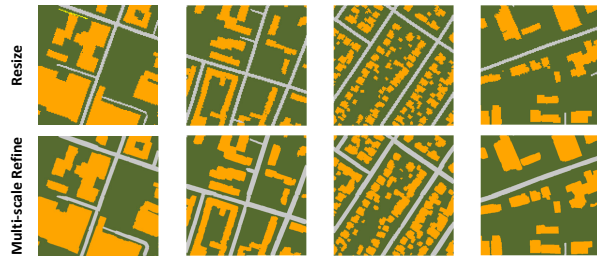


Figure 7. **Multi-scale Refinement.** (Top) When the original global patch (128×128) is resized to 512×512 , sawtooth patterns become apparent. (Below) After refinement, the results become smoother.

these priors would help them in the correct data estimation.

More Qualitative Results We demonstrate more qualitative results for other submodules. In Figure 5, we show outpainting examples for expanding local block layouts into global layouts. In Figure 7 we show effectiveness of multi-scale refinement, in Figure 9 we show the generated 3D layouts, and in Figure 8 we show rendered city scene images.

6. Ablation Study

Effectiveness of Training in One-hot Space In this section, we demonstrate the effectiveness of training the block generation models in one-hot space. Using the same set of training images and training techniques, we train the three-

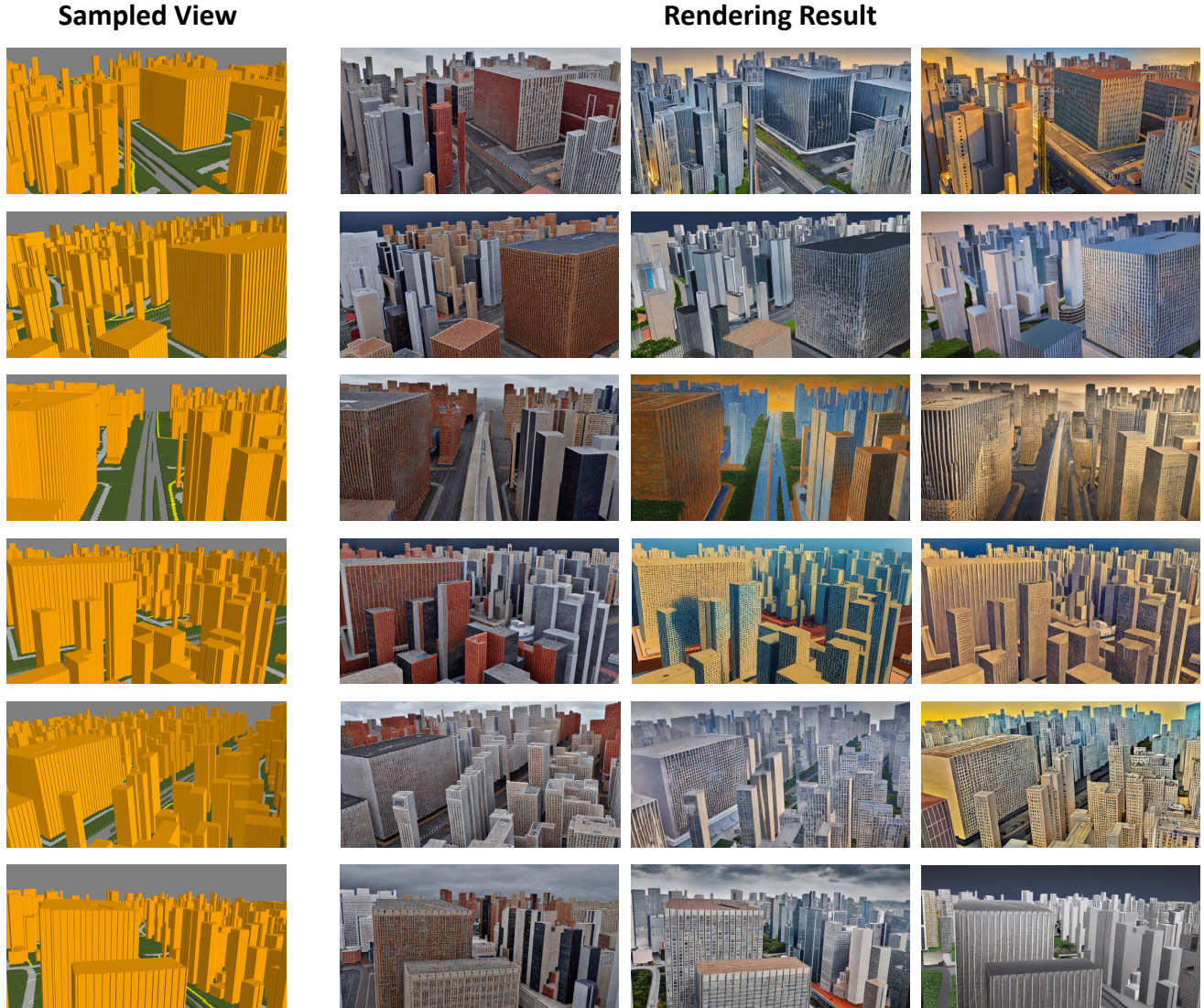


Figure 8. **The Render Results.** The first column are the input sampled views from our 3D layouts. The other columns are rendered results. Given sampled views of the generated 3D layouts, we can get realistic and diversified synthesis results.

Model \ Scale	128	256	512
BG	20.18 / 0.0221	28.92 / 0.0272	61.38 / 0.0595
BG _{whole}	28.35 / 0.0279	37.88 / 0.0380	75.72 / 0.0727
BG _{RGB}	56.15 / 0.0561	68.32 / 0.0656	85.13 / 0.0893

Table 3. FIDs / KIDs(\downarrow) for block generation models trained with images all scales, including our block generation models trained with data cleaning in one-hot space (BG), trained without data cleaning in one-hot space (BG_{whole}), and trained with data cleaning in RGB space (BG_{RGB}).

block generation models in RGB space and compare them with the block generation models trained in one-hot space. During sampling, we map the RGB values of samples back

to their nearest neighbors in the predefined palette. We compare the FIDs and KIDs with the results from block generation models trained in one-hot space in Table 3. We conclude that training in one-hot space can significantly boost the performance of block generation models.

Significance of Data Cleaning During training and testing, we observe that low-quality images in the training set would affect model training and degrade the quality of synthesized results, especially for models trained with images at lower resolutions. Specifically, if a 128×128 region is mostly covered by water or vegetation, it carries little semantic meaning and such low-quality training samples would impede the model’s capacity to accurately capture

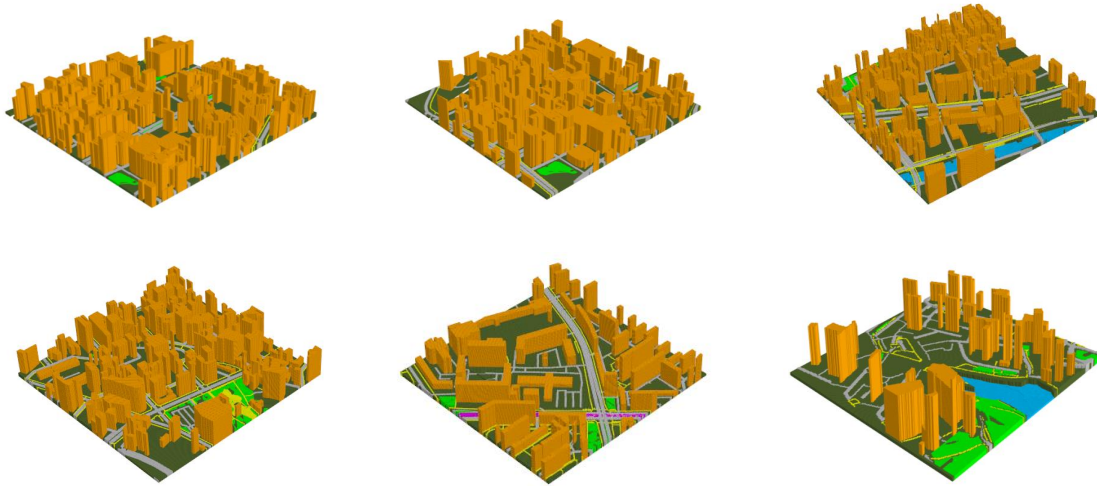


Figure 9. **Examples of Constructed 3D Layouts.** With generated semantic fields and synthesized height fields, we can construct high-quality 3D layouts.

the underlying distribution of the data. Therefore, we perform data cleaning to training images at all scales by both manually filtering and setting thresholds to some classes. For instance, an image is classified as a low-quality image and would be filtered if it satisfy any of the conditions: buildings $< 20\%$, water $> 30\%$, or rail $> 10\%$, *etc.* In Table 3 and we list FIDs and KIDs of models trained without data cleaning. The results suggest that the utilization of a filtered dataset in training yields a substantial improvement in the performance of block generation models.

7. Limitations and Future Work

Currently, we only sampled city scene images from limited views. For future work, addressing this limitation would involve exploring and implementing advanced rendering methodologies to enhance the model’s capacity for generating more accurate and consistent representations of urban environments.

8. Conclusion

In this paper, we introduce CityGen, a novel framework for 3D city layout synthesis. CityGen excels in generating infinite, diverse, and high-resolution city layouts that respond to user inputs. Our extensive experiments demonstrate that CityGen surpasses existing methods in quality and diversity of the generated layouts, while offering enhanced user control in the generation process. This approach significantly advances the field of urban design and 3D modeling, offering a valuable tool for professionals and enthusiasts in creating realistic and varied urban landscapes. For future work, we aim to provide more guidance in terms of user control, including the integration of text prompts for

more intuitive and specific layout generation. Additionally, we plan to extend our framework to support dynamic elements like moving vehicles and pedestrians.

References

- [1] Blender. <https://www.blender.org/>. 5
- [2] Esri’s cityengine. <https://www.esri.com/en-us/arcgis/products/arcgis-cityengine/overview>. 2
- [3] Openstreetmap. <https://www.openstreetmap.org/>. 4, 5
- [4] Unreal engine. <https://www.unrealengine.com/>. 2
- [5] Daniel G Aliaga, Carlos A Vanegas, and Bedrich Benes. Interactive example-based urban layout synthesis. *ACM transactions on graphics (TOG)*, 27(5):1–10, 2008. 1
- [6] Omri Avrahami, Dani Lischinski, and Ohad Fried. Blended diffusion for text-driven editing of natural images. In *Proceedings of the IEEE/CVF Conference on Computer Vision and Pattern Recognition*, pages 18208–18218, 2022. 4
- [7] Edmund N Bacon. *Design of cities: Revised edition*. Penguin books, 1976. 2
- [8] Mikolaj Bińkowski, Danica J Sutherland, Michael Arbel, and Arthur Gretton. Demystifying mmd gans. *arXiv preprint arXiv:1801.01401*, 2018. 6
- [9] Holger Caesar, Varun Bankiti, Alex H Lang, Sourabh Vora, Venice Erin Liong, Qiang Xu, Anush Krishnan, Yu Pan, Giancarlo Baldan, and Oscar Beijbom. nuscnets: A multi-modal dataset for autonomous driving. In *Proceedings of the IEEE/CVF conference on computer vision and pattern recognition*, pages 11621–11631, 2020. 2
- [10] Peter Calthorpe and William B Fulton. *The regional city: Planning for the end of sprawl*, volume 18. Island Press Washington, DC, 2001. 2
- [11] Shidong Cao, Wenhao Chai, Shengyu Hao, and Gaoang Wang. Image reference-guided fashion design with structure-aware transfer by diffusion models. In *Proceedings of the IEEE/CVF Conference on Computer Vision and Pattern Recognition*, pages 3524–3528, 2023. 1
- [12] Shidong Cao, Wenhao Chai, Shengyu Hao, Yanting Zhang, Hangyue Chen, and Gaoang Wang. Diffashion: Reference-based fashion design with structure-aware transfer by diffusion models. *arXiv preprint arXiv:2302.06826*, 2023. 1
- [13] Lucy Chai, Richard Tucker, Zhengqi Li, Phillip Isola, and Noah Snavely. Persistent nature: A generative model of unbounded 3d worlds. In *Proceedings of the IEEE/CVF Conference on Computer Vision and Pattern Recognition*, pages 20863–20874, 2023. 2
- [14] Wenhao Chai, Xun Guo, Gaoang Wang, and Yan Lu. Stable-video: Text-driven consistency-aware diffusion video editing. In *Proceedings of the IEEE/CVF International Conference on Computer Vision*, pages 23040–23050, 2023. 2
- [15] Eric R Chan, Connor Z Lin, Matthew A Chan, Koki Nagano, Boxiao Pan, Shalini De Mello, Orazio Gallo, Leonidas J Guibas, Jonathan Tremblay, Sameh Khamis, et al. Efficient geometry-aware 3d generative adversarial networks. In *Proceedings of the IEEE/CVF Conference on Computer Vision and Pattern Recognition*, pages 16123–16133, 2022. 2
- [16] Huiwen Chang, Han Zhang, Lu Jiang, Ce Liu, and William T Freeman. Maskgit: Masked generative image transformer. In *Proceedings of the IEEE/CVF Conference on Computer Vision and Pattern Recognition*, pages 11315–11325, 2022. 7
- [17] Guoning Chen, Gregory Esch, Peter Wonka, Pascal Müller, and Eugene Zhang. Interactive procedural street modeling. In *ACM SIGGRAPH 2008 papers*, pages 1–10. 2008. 1
- [18] Meida Chen, Qingyong Hu, Zifan Yu, Hugues Thomas, Andrew Feng, Yu Hou, Kyle McCullough, Fengbo Ren, and Lucio Soibelman. Stpls3d: A large-scale synthetic and real aerial photogrammetry 3d point cloud dataset. *arXiv preprint arXiv:2203.09065*, 2022. 2
- [19] Zhaoxi Chen, Guangcong Wang, and Ziwei Liu. Scenedreamer: Unbounded 3d scene generation from 2d image collections. *arXiv preprint arXiv:2302.01330*, 2023. 2
- [20] Zhaoxi Chen, Guangcong Wang, and Ziwei Liu. Scenedreamer: Unbounded 3d scene generation from 2d image collections. In *arXiv*, 2023. 2
- [21] Terrance DeVries, Miguel Angel Bautista, Nitish Srivastava, Graham W Taylor, and Joshua M Susskind. Unconstrained scene generation with locally conditioned radiance fields. In *Proceedings of the IEEE/CVF International Conference on Computer Vision*, pages 14304–14313, 2021. 2
- [22] Lubin Fan, Przemyslaw Musialski, Ligang Liu, and Peter Wonka. Structure completion for facade layouts. *ACM Trans. Graph.*, 33(6):210–1, 2014. 1
- [23] Lin Gao, Jia-Mu Sun, Kaichun Mo, Yu-Kun Lai, Leonidas J Guibas, and Jie Yang. Scenehgn: Hierarchical graph networks for 3d indoor scene generation with fine-grained geometry. *IEEE Transactions on Pattern Analysis and Machine Intelligence*, 2023. 2
- [24] M Ghorbanian and F Shariatpour. Procedural modeling as a practical technique for 3d assessment in urban design via cityengine. *Int. J. Architect. Eng. Urban Plan*, 29(2):255–267, 2019. 2
- [25] Saskia A Groenewegen, Ruben M Smelik, Klaas Jan de Kraker, and Rafael Bidarra. Procedural city layout generation based on urban land use models. *Short Paper Proceedings of Eurographics 2009*, 2009. 2
- [26] Zekun Hao, Arun Mallya, Serge Belongie, and Ming-Yu Liu. Gancraft: Unsupervised 3d neural rendering of minecraft worlds. In *Proceedings of the IEEE/CVF International Conference on Computer Vision*, pages 14072–14082, 2021. 2
- [27] Liu He, Yijuan Lu, John Corring, Dinei Florencio, and Cha Zhang. Diffusion-based document layout generation. *arXiv preprint arXiv:2303.10787*, 2023. 2
- [28] Olof Henricsson, Andre Streilein, and Armin Gruen. Automated 3-d reconstruction of buildings and visualization of city models, 1996. 1
- [29] Martin Heusel, Hubert Ramsauer, Thomas Unterthiner, Bernhard Nessler, and Sepp Hochreiter. Gans trained by a two time-scale update rule converge to a local nash equilibrium. *Advances in neural information processing systems*, 30, 2017. 6
- [30] Jonathan Ho, Ajay Jain, and Pieter Abbeel. Denoising diffusion probabilistic models. *Advances in neural information processing systems*, 33:6840–6851, 2020. 2, 5

- [31] Edward J Hu, Yelong Shen, Phillip Wallis, Zeyuan Allen-Zhu, Yuanzhi Li, Shean Wang, Lu Wang, and Weizhu Chen. Lora: Low-rank adaptation of large language models. *arXiv preprint arXiv:2106.09685*, 2021. [2](#), [4](#)
- [32] Qingyong Hu, Bo Yang, Sheikh Khalid, Wen Xiao, Niki Trigoni, and Andrew Markham. Towards semantic segmentation of urban-scale 3d point clouds: A dataset, benchmarks and challenges. In *Proceedings of the IEEE/CVF conference on computer vision and pattern recognition*, pages 4977–4987, 2021. [2](#)
- [33] Naoto Inoue, Kotaro Kikuchi, Edgar Simo-Serra, Mayu Otani, and Kota Yamaguchi. Layoutdm: Discrete diffusion model for controllable layout generation. In *Proceedings of the IEEE/CVF Conference on Computer Vision and Pattern Recognition*, pages 10167–10176, 2023. [2](#)
- [34] Akash Abdu Jyothi, Thibaut Durand, Jiawei He, Leonid Sigal, and Greg Mori. Layoutvae: Stochastic scene layout generation from a label set. In *Proceedings of the IEEE/CVF International Conference on Computer Vision*, pages 9895–9904, 2019. [2](#)
- [35] Byung-soo Kim, Pushmeet Kohli, and Silvio Savarese. 3d scene understanding by voxel-crf. In *Proceedings of the IEEE International Conference on Computer Vision*, pages 1425–1432, 2013. [2](#)
- [36] Diederik P Kingma and Jimmy Ba. Adam: A method for stochastic optimization. *arXiv preprint arXiv:1412.6980*, 2014. [5](#)
- [37] J Li, J Yang, A Hertzmann, J Zhang, and T Layoutgan Xu. Generating graphic layouts with wireframe discriminators. *arXiv preprint arXiv:1901.06767*, 2019. [2](#)
- [38] Yixuan Li, Lihan Jiang, Linning Xu, Yuanbo Xiangli, Zhenzhi Wang, Dahua Lin, and Bo Dai. Matrixcity: A large-scale city dataset for city-scale neural rendering and beyond. In *Proceedings of the IEEE/CVF International Conference on Computer Vision*, pages 3205–3215, 2023. [2](#), [4](#), [5](#)
- [39] Yiming Li, Zhiding Yu, Christopher Choy, Chaowei Xiao, Jose M Alvarez, Sanja Fidler, Chen Feng, and Anima Anandkumar. Voxformer: Sparse voxel transformer for camera-based 3d semantic scene completion. In *Proceedings of the IEEE/CVF Conference on Computer Vision and Pattern Recognition*, pages 9087–9098, 2023. [2](#)
- [40] Zhengqi Li, Qianqian Wang, Noah Snavely, and Angjoo Kanazawa. Infinitenature-zero: Learning perpetual view generation of natural scenes from single images. In *European Conference on Computer Vision*, pages 515–534. Springer, 2022. [2](#)
- [41] Yiyi Liao, Jun Xie, and Andreas Geiger. Kitti-360: A novel dataset and benchmarks for urban scene understanding in 2d and 3d. *IEEE Transactions on Pattern Analysis and Machine Intelligence*, 45(3):3292–3310, 2022. [2](#)
- [42] Chieh Hubert Lin, Hsin-Ying Lee, Yen-Chi Cheng, Sergey Tulyakov, and Ming-Hsuan Yang. Infinitygan: Towards infinite-pixel image synthesis. *arXiv preprint arXiv:2104.03963*, 2021. [6](#)
- [43] Chieh Hubert Lin, Hsin-Ying Lee, Willi Menapace, Menglei Chai, Aliaksandr Siarohin, Ming-Hsuan Yang, and Sergey Tulyakov. Infincity: Infinite-scale city synthesis. *arXiv preprint arXiv:2301.09637*, 2023. [2](#), [4](#), [6](#)
- [44] Markus Lipp, Daniel Scherzer, Peter Wonka, and Michael Wimmer. Interactive modeling of city layouts using layers of procedural content. In *Computer Graphics Forum*, volume 30, pages 345–354. Wiley Online Library, 2011. [1](#)
- [45] Andrew Liu, Richard Tucker, Varun Jampani, Ameesh Makadia, Noah Snavely, and Angjoo Kanazawa. Infinite nature: Perpetual view generation of natural scenes from a single image. In *Proceedings of the IEEE/CVF International Conference on Computer Vision*, pages 14458–14467, 2021. [2](#)
- [46] Marc Olano, Kurt Akeley, John C Hart, Wolfgang Heidrich, Michael McCool, Jason L Mitchell, and Randi Rost. Real-time shading. In *ACM SIGGRAPH 2004 Course Notes*, pages 1–es. 2004. [4](#)
- [47] Yichen Ouyang, Wenhao Chai, Jiayi Ye, Dapeng Tao, Yibing Zhan, and Gaoang Wang. Chasing consistency in text-to-3d generation from a single image. *arXiv preprint arXiv:2309.03599*, 2023. [2](#)
- [48] Yoav IH Parish and Pascal Müller. Procedural modeling of cities. In *Proceedings of the 28th annual conference on computer graphics and interactive techniques*, pages 301–308, 2001. [1](#)
- [49] Daniel Ritchie, Kai Wang, and Yu-an Lin. Fast and flexible indoor scene synthesis via deep convolutional generative models. In *Proceedings of the IEEE/CVF conference on computer vision and pattern recognition*, pages 6182–6190, 2019. [2](#)
- [50] Robin Rombach, Andreas Blattmann, Dominik Lorenz, Patrick Esser, and Björn Ommer. High-resolution image synthesis with latent diffusion models. In *Proceedings of the IEEE/CVF conference on computer vision and pattern recognition*, pages 10684–10695, 2022. [2](#), [4](#)
- [51] Olaf Ronneberger, Philipp Fischer, and Thomas Brox. U-net: Convolutional networks for biomedical image segmentation. In *Medical Image Computing and Computer-Assisted Intervention—MICCAI 2015: 18th International Conference, Munich, Germany, October 5–9, 2015, Proceedings, Part III 18*, pages 234–241. Springer, 2015. [5](#)
- [52] Yuan Shen, Wei-Chiu Ma, and Shenlong Wang. Sgam: Building a virtual 3d world through simultaneous generation and mapping. *Advances in Neural Information Processing Systems*, 35:22090–22102, 2022. [2](#)
- [53] Zifan Shi, Yujun Shen, Jiapeng Zhu, Dit-Yan Yeung, and Qifeng Chen. 3d-aware indoor scene synthesis with depth priors. In *European Conference on Computer Vision*, pages 406–422. Springer, 2022. [2](#)
- [54] Jerry O Talton, Yu Lou, Steve Lesser, Jared Duke, Radomir Mech, and Vladlen Koltun. Metropolis procedural modeling. *ACM Trans. Graph.*, 30(2):11–1, 2011. [1](#)
- [55] Matthew Tancik, Vincent Casser, Xinchen Yan, Sabeek Pradhan, Ben Mildenhall, Pratul P Srinivasan, Jonathan T Barron, and Henrik Kretschmar. Block-nerf: Scalable large scene neural view synthesis. In *Proceedings of the IEEE/CVF Conference on Computer Vision and Pattern Recognition*, pages 8248–8258, 2022. [2](#)
- [56] Wenwen Tong, Chonghao Sima, Tai Wang, Li Chen, Silei Wu, Hanming Deng, Yi Gu, Lewei Lu, Ping Luo, Dahua Lin,

- et al. Scene as occupancy. In *Proceedings of the IEEE/CVF International Conference on Computer Vision*, pages 8406–8415, 2023. [2](#)
- [57] Haithem Turki, Deva Ramanan, and Mahadev Satyanarayanan. Mega-nerf: Scalable construction of large-scale nerfs for virtual fly-throughs. In *Proceedings of the IEEE/CVF Conference on Computer Vision and Pattern Recognition*, pages 12922–12931, 2022. [2](#)
- [58] Vladimir Vezhnevets, Anton Konushin, and Alexey Ignatenko. Interactive image-based urban modeling. In *Proc. of PIA*, pages 63–68, 2007. [1](#)
- [59] Yuqi Wang, Yuntao Chen, Xingyu Liao, Lue Fan, and Zhaoxiang Zhang. Panoocc: Unified occupancy representation for camera-based 3d panoptic segmentation. *arXiv preprint arXiv:2306.10013*, 2023. [2](#)
- [60] Yuanbo Xiangli, Linning Xu, Xingang Pan, Nanxuan Zhao, Anyi Rao, Christian Theobalt, Bo Dai, and Dahua Lin. Bungeenerf: Progressive neural radiance field for extreme multi-scale scene rendering. In *European conference on computer vision*, pages 106–122. Springer, 2022. [2](#)
- [61] Haozhe Xie, Zhaoxi Chen, Fangzhou Hong, and Ziwei Liu. Citydreamer: Compositional generative model of unbounded 3d cities. *arXiv preprint arXiv:2309.00610*, 2023. [2](#), [4](#), [6](#), [7](#)
- [62] Yong-Liang Yang, Jun Wang, Etienne Vouga, and Peter Wonka. Urban pattern: Layout design by hierarchical domain splitting. *ACM Transactions on Graphics (TOG)*, 32(6):1–12, 2013. [1](#)
- [63] Lvmin Zhang, Anyi Rao, and Maneesh Agrawala. Adding conditional control to text-to-image diffusion models. In *Proceedings of the IEEE/CVF International Conference on Computer Vision*, pages 3836–3847, 2023. [2](#), [5](#)